Journal of Applied Polymer Science

Morphology and thermal properties of recycled polyacrylonitrile fiber blends with poly(ethylene terephthalate): Microstructural characterization

Taoreed Adesola Adegbola,[1,2] Sadiku E. Rotimi,[1,2] Sinha Ray Suprakas[3,4]

[1]Department of Mechanical Engineering, Faculty of Engineering and the Built Environment, Tshwane University of Technology, Pretoria 0001, South Africa

[2]Department of Chemical Engineering, Faculty of Engineering and the Built Environment, Tshwane University of Technology, Pretoria 0001, South Africa

[3]DST-CSIR National Centre for Nanostructured Materials, Council for Scientific and Industrial Research, Pretoria 0001, South Africa

[4]Department of Applied Chemistry, University of Johannesburg, Doornfontein 2028, South Africa

Correspondence to: T. A. Adegbola (E-mail: adesolaat@tut.ac.za)

ABSTRACT: The compounding of rPAN/PET [polyacrylonitrile/poly(ethylene terephthalate]; 30/70, 50/50, and 70/30 wt %) using a melt-blending technique was the main focus of this investigation. An X-ray diffraction study indicated the possibility of interphase boundary interactions between the polymer matrices in the blends. The differential scanning calorimetry results showed that varying the ratios of rPAN in the blends marginally improved the processing temperature of PET. The thermogravimetric analysis revealed that the addition of PET up to 70% increased the thermal stability of the blend, and adding more than 70% of PET resulted in poor adhesion between the matrix and phase. On the basis of the results obtained, we propose a general understanding of how the morphology and the mechanical and thermal properties of the blend could assist in the development of rPAN blends with PET, rather than disposing of the viable materials as wastes. © 2016 Wiley Periodicals, Inc. J. Appl. Polym. Sci. **2016**, *133*, 43777.

KEYWORDS: blends; crystallization; differential scanning calorimetry (DSC); mechanical properties; morphology

Received 10 November 2015; accepted 8 April 2016

DOI: 10.1002/app.43777

INTRODUCTION

Polyacrylonitrile (PAN) and poly(ethylene terephthalate) (PET) are widely sought polymers that have been successfully used to develop several commercial and industrial products in the textile, automobile, food, packaging, and filtration industries.[1,2] Disposal of PAN fiber that has been used as a filtration material is of great environmental concern and needs to be addressed through recycling. Over the years, increased research on polymer development has been undertaken in order to improve on the recycling of the readily available polymeric materials because of environmental concerns and government legislations. Therefore, suitable compounding methods through improved polymer processing techniques with acceptable blending ratios of recycled PAN (rPAN)/PET need to be explored in order to obtain useful and serviceable blends, although processing challenges like variations in the thermal properties of the blended polymers can be a determining factor. Hence, varying the compositional ratios of the blends might improve the thermal stability of the blended polymers. Therefore, understanding the effect of varying blending ratios is highly important in improving the blend properties, and this is worth exploring. A significant amount of research has shown the blending prospects of PAN and PET. Kim *et al.*[3] worked on PAN that was modified by copolymerizing with methyl acrylate (MA) and 2-acrylamido-2-methyl propane sulfonic acid (AMPS, also abbreviated as AP) and blended with cellulose acetate (CA) in dimethyl formamide (80/20, 60/40, 40/60, and 20/80 by weight). The results from solution blends of the two types of modified PAN with CA showed partial miscibility, as evidenced by the inward migration of the two glass-transition temperatures (T_g). The migration of T_g was much greater with PAN than with CA, an indication of greater solubility of CA in PAN, a result consistent with the conjugate phase calculations. Their SEM micrographs showed that phase inversion occurred at 60/40 for MA–PAN–CA and 40/60 for AP–PA–CA blends, the compositions corresponding to the tensile strength minimum and predicted by the Coran–Patel model. Peebles *et al.*[4] studied the thermal degradation of

© 2016 Wiley Periodicals, Inc.

PAN under inert atmospheric conditions. They concluded that PAN can be transformed into a more stable material by prolonged heating at 225 °C.

Zhu *et al.*[5] studied the properties of poly(vinyl alcohol) (PVA)/PAN blended films. The results showed that the introduction of PAN could exert marked effects on the properties of PVA films. Seydibeyoglu[6] studied a partially biobased PAN/lignin blend as a potential carbon fiber precursor. The results showed that it is possible to develop a new precursor material with a blend of lignin and PAN. The study also demonstrated a new application area of lignin, which is an undervalued coproduct of many industries. Furthermore, a partial replacement of PAN with a renewable resource and making the PAN precursor greener are envisaged to improve the world environment.

Feng *et al.*[7] worked on enhancing the mechanical and thermal properties of PAN by blending it with tea polyphenol (TP). Their results revealed that PAN/TP made with 12.5 wt % TP had a better antiwear ability and a hardness similar to that of *acrylonitrile butadiene styrene* (ABS). In addition, all the PAN/TP blends prepared showed lower impact strength than the referenced ABS. Finally, the blends revealed enhanced thermal stability when compared to the pure PAN.

Mendes *et al.*[8] studied the effect of the reaction temperature on the thermal, morphological, and viscosity properties of solid-state polymerized PET/Polycarbonate (PC) extruded blends. Their result revealed that after the solid-state polymerization, at all reaction temperatures, the PET glass-transition and crystallization temperatures slightly decreased, the melting temperature marginally increased, and the degree of crystallinity was practically unaffected. In addition, their result revealed the appearance of structures such as bridges linking the matrix and the dispersed domains. These bridges were correlated to the PET/PC block copolymer obtained through blending in the molten state.

Ujhelyiová *et al.*[9] worked on polypropylene (PP)/PET blended fibers and focused mainly on the crystallization behavior of PP and the mechanical properties of the blends. They observed that the heating and cooling rates influenced the thermal properties of the PP/PET fibers. In addition, the tensile strength and elongation at break of the blended PP/PET fibers changed under the influence of PET and compatibilizer.

Szostak[10] studied the mechanical and thermal properties of PET/poly(butylene terephthalate) (PBT) blends. His result showed that PET/PBT blends were processable by injection molding only, following mixing on an extrusion machine and subsequent injection molding of the blends. It was observed that the manner of preparation of the blends had the greatest influence on their mechanical properties, especially on the impact strength. The study also revealed that the mixing of PET and PBT only during the injection molding is not sufficient to yield the expected and essential improvement of the impact resistance of the PET/PBT blends. Therefore, in order to guarantee the enhanced properties of the injected PET/PBT blends, it is necessary to first mix them on the extrusion machine.

Di Lorenzo *et al.*[11] successfully polymerized PET with $CaCO_3$ coated with stearic acid and uncoated. They found that coated $CaCO_3$ resulted in a stronger polymer–filler interaction when compared to the uncoated particle. The strong interfacial adhesion between the phases resulted in a significant increase of the glass-transition temperature by 14 °C and the melting temperature by 8 °C when compared with neat PET.

Literature on PAN/PET blends is unavailable, and hence success has been limited on the recycling and the compatibility of PAN with PET. Therefore, this study is needed. The main focus of this report is on the recycling of used PAN fiber blended with PET at different ratios. The essence is to establish a relationship between morphology and the obtained thermal properties. The PAN fiber employed in this study was previously used as coal and fly ash filtrating material in power-generating plants.

EXPERIMENTAL

Materials

The rPAN fiber employed in this study was supplied by ESKOM (Sunninghill, South Africa). Neat PAN has a molecular weight of the repeat unit (M_w) = 53.06 g/mol and an amorphous density of 1.184 g/cm^3. The glass-transition and melting temperatures of PAN are 95 °C and 317 °C, respectively. The PET was purchased by the Tshwane University of Technology (TUT) from Ten Cate Advanced Composites BV (Nijverdal, The Netherlands). PET has a molecular weight of the repeat unit (M_w) = 192.2 g/mol and an amorphous density of 1.370 g/cm^3. The glass-transition and melting temperatures are 75 °C and 285 °C, respectively.

The Recycled PAN Fiber and PET Processing

rPAN fibers were cleaned by soaking in water for 12 h, rinsed, and dried for 24 h at room temperature in order to remove the ash and coal particles embedded in them before the blending process took place. Dried rPAN fibers and neat PET were prepared through melt-blending using the HAAKE Polylab OS Rheomix 600 (Thermo Electron Co., Beverly) at 290 °C for 5 min with a rotor speed of 80 rpm. The rPAN and PET were blended in the ratios 30/70, 50/50, and 70/30, while rPAN and PET were used as controls. The resulting blends and control samples were molded into the desired dimensions for various tests (ASTM). A Carver compression mold (Carver, Wabash) technique was used for the samples with a residence time of 10 min in steps of 2 min at a pressure of 1 metric ton, and water was used for the slow cooling during the carving process.

CHARACTERIZATION

Differential Scanning Calorimetry (DSC)

A DSC study was performed using instrument DSC (Pittsburgh) Q2000 V24.4 Build 116, Module DSC standard cell RC, set at a temperature between −50 and 290 °C for all the samples. Three DSC experiment profiles were applied in order to study the thermal properties of the rPAN/PET blended samples. The first involved a conventional scan, where the samples were heated from −50 °C to 290 °C and held at 290 °C for 5 min in order to eliminate the previous thermal history. The samples were then cooled to 0 °C and reheated to 290 °C. Both heating and cooling steps were performed at 10 °C/min.

An isothermal DSC scan profile was used to determine the crystallization of the blends. In this profile, the samples (4.940 mg)

were heated from −50 °C to 290 °C at a rate of 10 °C/min and held for 5 min. The samples were then equilibrated to 200 °C and held isothermally for 10 min. The heat flow rate of the samples was recorded until the baseline was recovered and the sample's crystallization was attained.

Thermogravimetric Analysis (TGA)

TGA was performed using Instrument TGA Q500 V20.10 Build 36 module TGA, TA Instruments (New Castle, USA). A temperature ramp with a heating rate of 10 °C/min up to 900 °C from 0 °C was used. TGA provides information on the sample's thermal characterization, degradation, moisture content, weight loss, and residue. This plays a vital role in the blend development.

X-ray Diffraction (XRD)

XRD patterns of rPAN, PET, and the blended samples were obtained using a PanAnalytical X'pertPRO diffractometer (PanAnalytical, Almelo, the Netherlands) (Cu Kα radiation; wavelength = 0.154 nm) with an operating voltage of 45 kV and current of 40 mA. Scanning was performed in the range 2θ = 0–80°, with a scanning step size of 0.0263° and a step time of 132.09 s. XRD investigates the polymer crystalline structure, which includes the atomic arrangement, crystallite size, lattice distortions, phase composition, orientation, and imperfection in the samples. All of these are highly important characterization parameters in the field of polymer-based material development for different applications.

Scanning Electron Microscopy (SEM)

The cryogenically fractured surface morphology of rPAN, PET, and the blended samples was determined using a JEOL-SEM model JSM-7500 field emission SEM (JEOL, Chuo-Ku, Tokyo, Japan). An accelerating voltage of 3 kV was used under the gentle beam (low mode) in order to prevent the beam from damaging the samples. The samples were prepared by immersing in liquid nitrogen, cryogenically fractured, mounted on stubs edge-on, and coated with mercury in order to enhance conductivity. The size of the distinct features of the images was determined using ImageJ software (National Institutes of Health, Bethesda). The images were collected at a magnification of 5×.

Impact Test

According to the ISO 179 standard, a Charpy impact test specimen with dimensions of approximately 80 × 10 × 4 mm (L × W × B) were compression-molded for the test. Using the CEAST Notchvis Plus (Piacenza, Italy), the polymer samples was notched on one side, with a notch root radius of 0.25 mm at 2 mm depth, while a CEAST Pendulum Resil Impactor II (Italy) at room temperature measured the notched Charpy impact strength (ISO 179). The hammer energy was 7.5 J with a drop velocity of 3.7 m/s, and 40 mm was the fixed span between supports for the tests. The results of the averages of six independent tests per sample are presented.

RESULTS AND DISCUSSION

Thermal Properties

The assessment of the thermal properties of rPAN/PET blends would aid in the understanding of the interaction between the two polymers. Figure 1 shows the DSC curves of rPAN, PET, and the blended samples. Figure 1(a–c) presents the second heating curves of rPAN, PET, and their blends, showing the

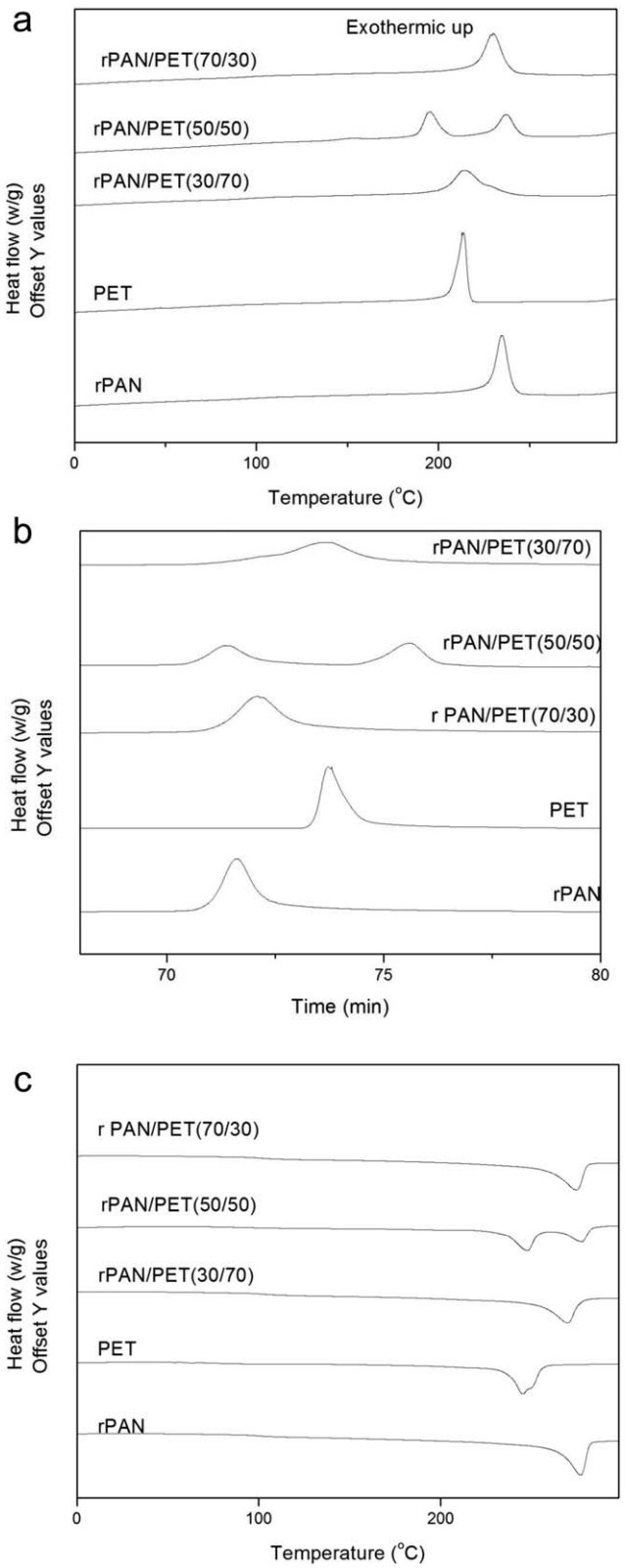

Figure 1. (a) DSC crystallization profiles of rPAN, PET, and blended rPAN/PET samples; second heating curves of the samples. (b) Heat flow during isothermal crystallization of rPAN; second heating curves of the samples. (c) Heat flow during isothermal crystallization of rPAN, PET, and blended rPAN/PET samples; second heating curves of the samples.

Table I. DSC Parameters of rPAN, PET, and rPAN/PET Blends

Samples	Peak crystallization temperature (°C)	Onset crystallization temperature (°C)	Peak melting temperature (°C)	Onset melting temperature (°C)	Enthalpy heat of crystallization (J/kg)	Enthalpy heat of melting (J/kg)	Degree of supercooling ΔT (°C)
rPAN	234.8	240.9	277.0	263.6	29.6	21.8	42.2
rPAN/PET (70/30)	237.4	244.8	277.5	266.6	16.7	8.9	40.1
rPAN/PET (50/50)	237.4	242.1	277.5	266.6	10.2	6.0	40.1
rPAN/PET (30/70)	234.1	242.1	277.7	266.6	5.3	3.0	43.6
PET	213.0	216.9	245.3	236.3	26.9	20.5	32.3

melting and crystallization peaks. The melting and crystallization values for rPAN, PET, and the blended samples show marginal increases (Table I). In addition to this observation, rPAN shows a crystallization exotherm earlier than PET (i.e., rPAN crystallized ~42.6 °C earlier than PET), indicating that rPAN is acting as a nucleating site for PET [Figure 1(a)]. Hence, the crystallinity and the rate of crystallization increased for PET in the blends, suggesting that high rPAN content will facilitate the crystallization of PET. Therefore, as the composition of PET increased, the number of PET crystals formed in the blend increased. In addition, a crystallization process occurring in the blended samples through a sequence of primary nucleation and a crystal growth mechanism was also observed through the degree of supercooling ($\Delta T = T_m - T_x$) result in Table I; this confirmed the discussion on crystallization.

Figure 1(b) also shows the isothermal crystallization curves of the samples (Table I). The time corresponding to the maximum peak (exotherm) was taken as the peak time of crystallization (t_{peak}). Such peaks are seen at different isothermal crystallization temperatures of rPAN, PET, and their blends, with the earlier crystallization corresponding to the lower isothermal crystallization temperature.

Furthermore, there are slight increases in the melting temperature of the blends when compared with rPAN and PET. The addition of PET in the composition improves the crystallinity of rPAN in the blend, as revealed by the reduction and shift to the left for both the melting and crystallization temperatures [Figure 1(c)]. This shift to lower temperature should assist in the processing of rPAN. The values for enthalpy heat of melting and crystallization, tabulated in Table I, are low for the blends of rPAN/PET (30/70 and 50/50) but highest in the blend rPAN/PET (70/30). This phenomenon is a result of the high rPAN content in this particular composition.

Table II. TGA Peak Temperatures of rPAN, PET, and rPAN/PET Blends

Blended samples	Peak temperature (°C)	Onset temperature (°C)	Char (%)
rPAN	643.5	464.9	4.74
rPAN/PET (70/30)	634.4 (rPAN) 415.1 (PET)	347.2	14.8
rPAN/PET (50/50)	614.8 (rPAN) 419.6 (PET)	356.5	21.0
rPAN/PET (30/70)	583.5 (rPAN) 421.3 (PET)	363.2	26.2
PET	423.7	352.5	35.9

Thermogravimetric Analysis (TGA)

The onset and peak degradation temperatures and the char formation are shown in Table II, and the curves for rPAN, PET, and the blends are shown in Figure 2. It was observed that both polymers decomposed individually in the blend. There are two independent decomposition peaks, indicating two stages of decomposition for the blended samples at temperatures ranging between 415 °C–421 °C and 583 °C–634 °C (Table II). The curves for the rPAN/PET blends showed a significant reduction in weight loss in comparison to the curves of rPAN and PET (Figure 2). This observation might be due to the breakdown and rearranging of the chains or bonds in the blends. In addition, the blends revealed the onset degradation temperature (T_{onset}) differences between rPAN and the blends to be 117 °C for rPAN/PET (70/30), 108 °C for rPAN/PET (50/50), and 101 °C for rPAN/PET (30/70). For PET and the blends, the onset degradation temperature differences are 5 °C for rPAN/PET (70/30), −4 °C for rPAN/PET (50/50), and −11 °C for rPAN/PET (30/70). Thus, from the changes in the onset degradation temperature values, PET influenced the thermal stability of rPAN in blends by lowering its onset degradation temperature. Furthermore, the addition of PET increases the processing temperature

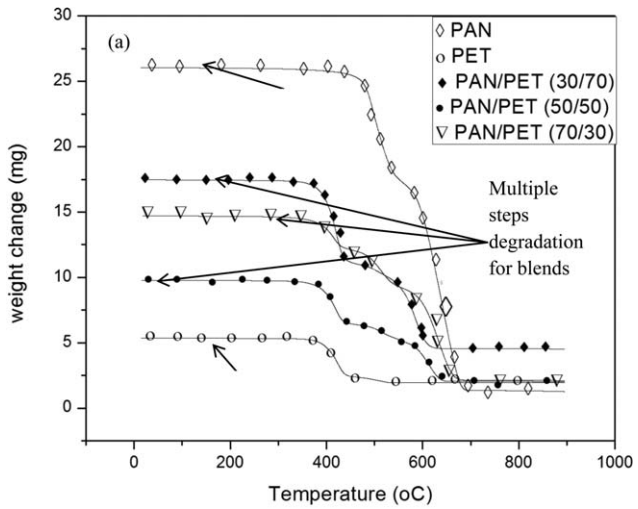

Figure 2. Weight-loss profiles.

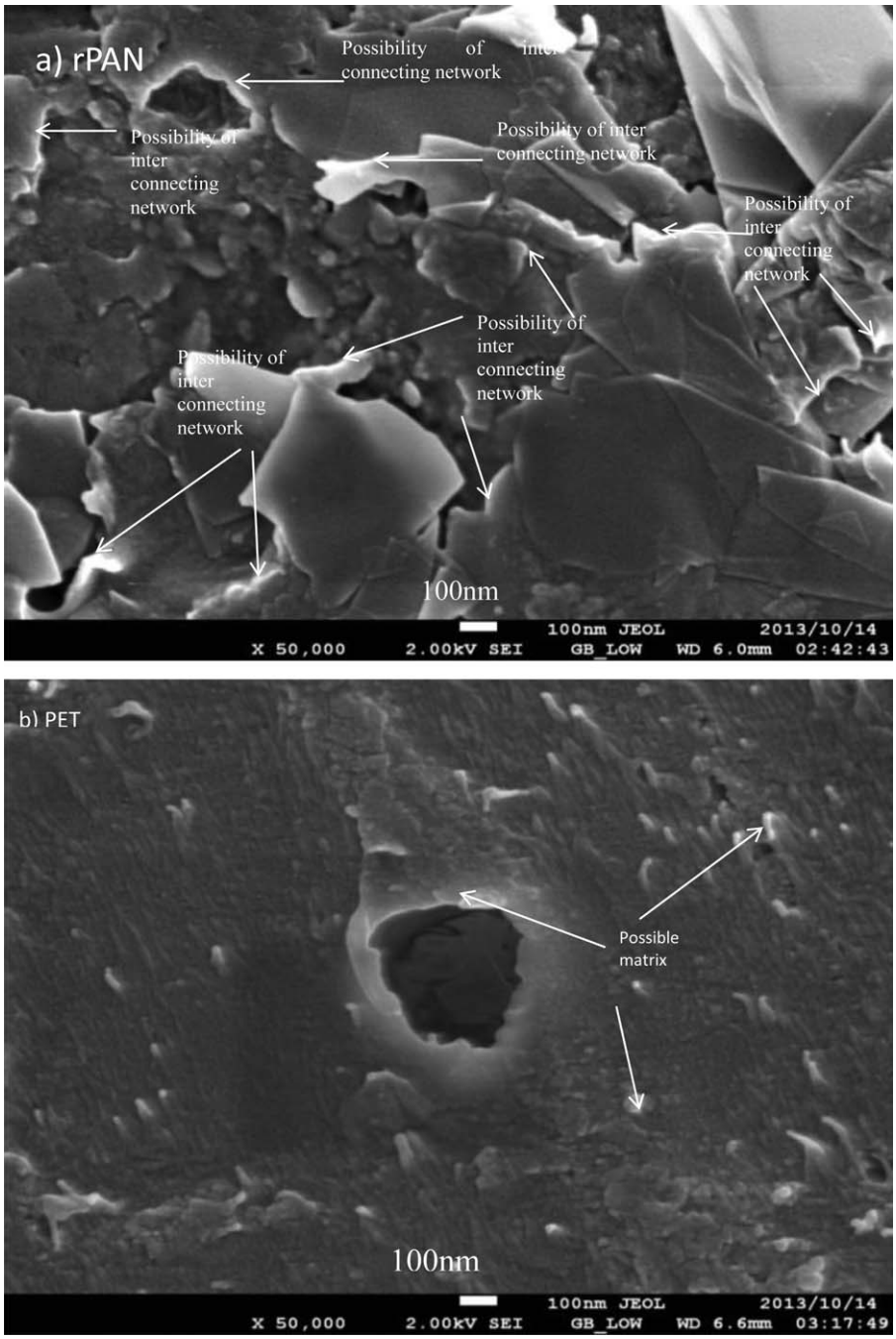

Figure 3. Morphology of freeze-fractured surfaces of (a) rPAN and (b) PET. Images were collected at 50,000× at a voltage of 2 kV.

of the blend because the temperature at which PET degraded increased with an increasing amount of rPAN in the blend. In addition, the blended samples revealed the percent char formation in the following order: 14.8%, 21%, and 26.2% for rPAN/PET (70/30, 50/50, 30/70) when compared to PET. These chars could be related to undecomposed PET within the range of processing temperatures.

Morphology

Figures 3 and 4 shows the cryogenically fractured SEM surfaces of rPAN, PET, and rPAN/PET blended samples. A phase-separated structure with a round to ovoid dispersed phase was observed in the blends. It is quite impossible to determine the sizes of the dispersed phases in the blended samples because of the nature of the blended polymers (the brown colors are inseparable). In a mixture of immiscible polymers, the presence of anisotropic nanoparticles in one of the polymer phases has been suggested to affect the morphology and properties of the polymers based on viscosity modification.[12] Hence, it is a well-proven fact that the miscibility of polymers depends greatly on their chemical interaction parameters. In the present work, the fraction of PET in the blend was bound to influence the

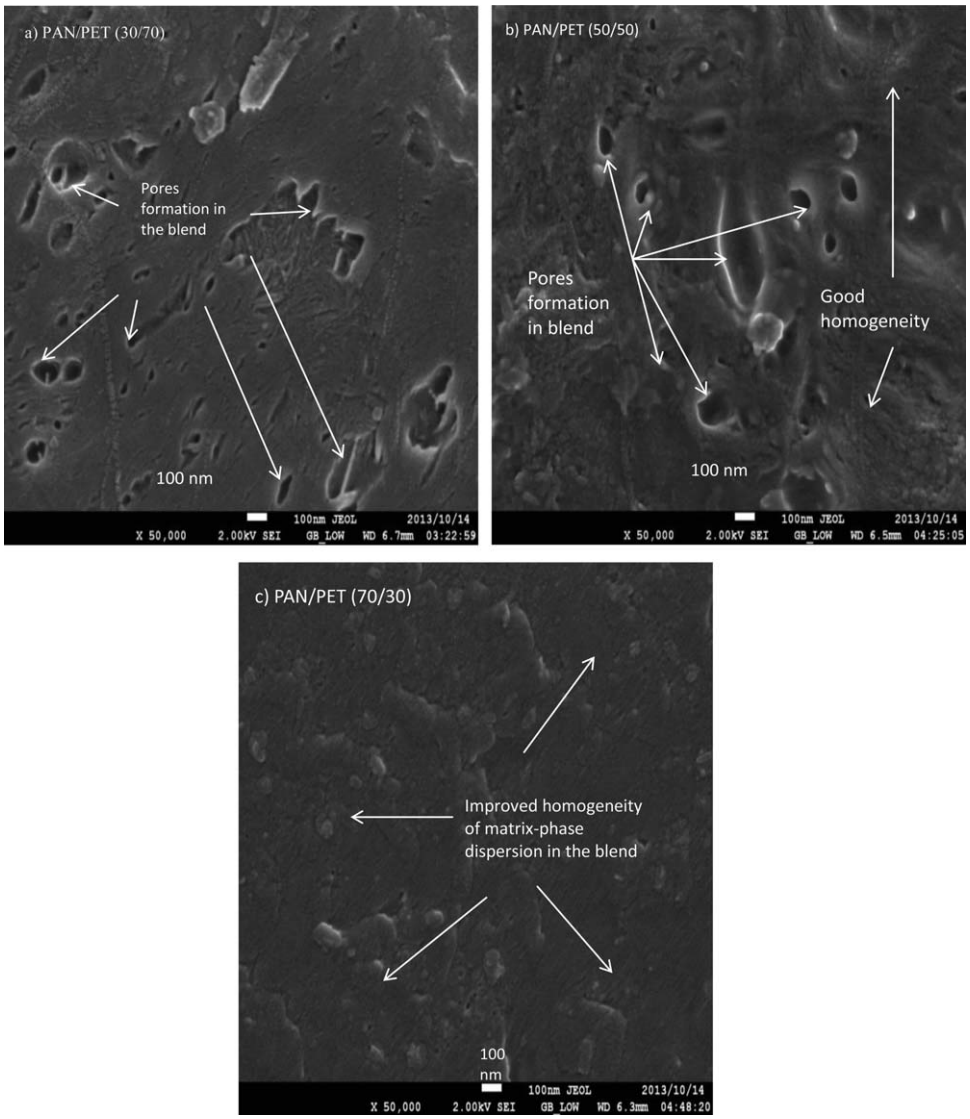

Figure 4. Morphology of freeze-fractured surfaces of rPAN/PET blends at different ratios (30/70, 50/50, and 70/30). The images were collected at 50,000× at a voltage of 2 kV.

viscosity of rPAN, and vice versa for PET. Therefore, the morphology of rPAN/PET blends was studied in order to elucidate the blend homogeneity or otherwise.

The micrograph of rPAN revealed a complex interconnected network of fibers (Figure 3). Obviously, the rPAN fiber morphology provides a compounding pathway that can enhance an effective blending. This can improve the properties of rPAN/PET blends if carefully explored. Figure 3 shows the morphology of the pure PET; this revealed possible matrix compounding for new material development. The morphology reveals the possibilities of fiber penetration in the network of the matrix; this is a positive prospect for rPAN fiber blending. The morphology of the rPAN/PET (30/70) sample is shown in Figure 4(a). The blend shows some degree of uniformity of the two polymers, but it further revealed the formation of pores in the blend, which resulted in matrix weakness, thereby leading to sample brittleness as a result of poor adhesion between the components. This ratio is not viable for recycling processes. Figure 4(b) reveals the morphology of the rPAN/PET (50/50) sample. The micrograph shows a cocontinuous morphology in the blend structure that contains some degree of interpenetrating and self-supporting phases of the rPAN/PET blend. This shows the continuous path through which either phase may be drawn to the boundaries, although some dispersed-phase portions were also observed in the blend. Lastly, Figure 4(c) shows the (70/30) blend of rPAN/PET. This blend reveals a near-total dispersion of PET in the rPAN matrix. This dispersion shows improved homogenization between the two polymers because the blend does not exhibit any distinguishable structural components.

XRD Study

The XRD intensity profiles of rPAN, PET, and blends of PAN/PET are shown in Figure 5. The XRD patterns of the blends (rPAN70/PET30, rPAN 30/PET70, and rPAN50/PET50) displayed the presence of peaks at $2\theta = 20.98°$, 26.49°, and 21.03°, corresponding to the crystal reflections (8587), (6679), and (6483), respectively. The rPAN and PET show peaks at

$2\theta = 20.07°$ and 26.57°, respectively, and their respective intensity counts are 10,983 and 7285.[13] The result shows that the (50/50) blend of rPAN/PET had the lowest intensity count. This crystalline structure of the polymer matrix plays a key role in determining the properties and development of the polymer-based blend system.[14,15]

The intensity of the peaks changes based on the compositional ratios of the blends (Figure 5). Therefore, the changes in the peak height might be related to the blends formed. In addition, rPAN/PET blends (Figure 5) also showed the shift toward a lower 2θ, revealing an increase in crystal formation in the blend; this shift can be explained considering three phenomena. The first phenomenon, suggested by Garbev *et al.*[16] and Beuchle *et al.*,[17] is that with increasing content of rPAN/PET ratio, the site occupancy of bridging matrix-phase chains may decrease. This decreases the occupancy of the structure space, thus allowing a reduction of the materials size-to-size distance through the action of blends. The second phenomenon is a decrease in the crystallite size along the c^* axis, that is, a decrease in the mean number of arranged structures. Such a decrease leads to a shift of the intensity of the reflection toward the low-angle region, which is exacerbated for the blends. This mainly originates from the fact that, in the low-angle region of XRD patterns, the Lorentz polarization factor strongly improves the shift toward the low-angle part, and thus this artificially displaces the diffraction peaks.[18–20]

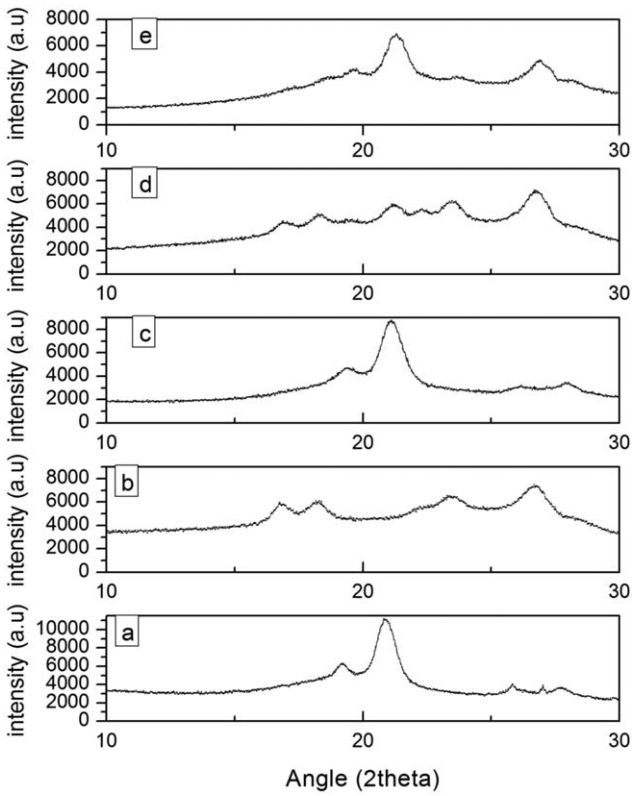

Figure 5. XRD diffraction patterns of (a) rPAN, (b) PET, (c) rPAN/PET (30/70), (d) rPAN/PET (50/50), and (e) rPAN/PET (70/30). The blends shift toward low 2θ. The broadening of width and changes in the blend intensity peaks are also revealed.

Table III. Impact Analysis Results

Samples	Absorbed energy (%)	Repeatability (Re) (kJ/m^2)	Energy (J)
rPAN	0.81	1.93	0.061
rPAN/PET (70/30)	0.90	1.90	0.068
rPAN/PET (50/50)	1.24	2.72	0.083
rPAN/PET (30/70)	The sample exhibited progressive cracks and broke during the notching process. It was very brittle.		
PET	1.23	2.63	0.093

The third hypothesis based on interstratification (i.e., the stacking along the c^* axis of at least two types of layers of contracting structural composition) may explain the shift toward low 2θ, based on the intensity of the reflection as a function of rPAN/PET ratio, which may be the interstratification from a region of low PET in the rPAN/PET blend with one of high PET in the rPAN/PET blend, the first being dominant for low structural rPAN/PET ratio, and vice versa.[19] Based on these phenomena, the formation of new phases that is due to the different ratios of rPAN and PET in the blends might have affected the types of crystals formed, which are very vital for blend development.

Impact Test

The sample impact test results are tabulated in Table III. The rPAN/PET (50/50) blend revealed high impact energy, followed by rPAN/PET (70/30), when compared with rPAN. This finding indicated that the addition of PET (up to 50%) improves the mechanical properties of rPAN. In addition to this finding, it was also observed that, at a slight notching impact on the blend of rPAN/PET (30/70), the sample cracked and could not be processed any further (see Table III). This shows that the blend is very brittle, and it reflects a very poor mechanical integrity that is due to the high composition of PET. The impact test finding is in agreement with the blend's crystal formation and its arrangement, as discussed in the SEM and XRD sections.

Correlation of the Results

DSC is used to understand the phase changes of the materials and also to determine the crystallinity of the materials. In contrast, XRD is used to characterize the crystal structure, phase, crystallinity, and so on. Therefore, it is of great importance to use XRD and DSC in characterizing the blends, as discussed in the sections on thermal properties and XRD. TGA provides the thermal degradation behavior, which can be linked (indirectly) to the morphology (SEM) of the blends in relation to the matrix and the dispersed phases present in the samples. Lastly, the morphology corroborates the impact test result. This information is vital in blend development.

CONCLUSIONS

The objective of this work was to study the recycling probability of used rPAN fiber blended with PET at different ratios and study the morphology and mechanical and thermal properties of the blended samples. From the findings, the ratios of PET in

the blend composition affect the thermal stability of rPAN and its impact strength. This was established from the thermal characterizations and morphological investigations, via DSC, SEM, TGA, and XRD. These provide important processing information (temperature) and microscopy information on rPAN/PET blends. It should also be noted that XRD and DSC studies provide important information on phase transitions, especially in the study of the correlation between microscopic structure, mechanical properties, and thermodynamic behavior. The XRD and DSC data complement each other in the understanding of the reaction processes. Also, the addition of equal amounts of PET and rPAN (50/50) revealed some degree of homogeneity in the composition. Lastly, the SEM study revealed a viable possibility of recycling used PAN fiber, and the addition of 70% and above of PET in the blended sample negatively affects the desirable property of the blend, resulting in a weak matrix and hence leading to brittleness. It is proposed that the addition of additives and fillers to the composition in order to improve the blend properties be explored, along with explorations of possible applications of blends of rPAN/PET.

REFERENCES

1. Cao, X.; Wang, X.; Ding, B.; Yu, J.; Sun, G. *Carbohydr. Polym.* **2013**, *92*, 2041.
2. Ghanbarzadeh, B.; Almasi, H. *Biodegrad. Polym.* **2013**.
3. Kim, B. K.; Oh, Y. S.; Lee, Y. M.; Lee, K. Y.; Soo, L. *J. Polym.* **2005**, *41*, 385.
4. Peebles, Jr., L. H.; Peters, W.; Snow, A.; Peyser, P. *Carbon* **1990**, *28*, 707.
5. Zhu, G.; Wang, F.; Xu, K.; Gao, Q.; Liu, Y. *Polímeros* **2013**, *23*, 146.
6. Seydibeyoglu, M. O. *J. Biomed. Biotechnol.* **2012**, *2012*, 1.
7. Feng, L.; Li, J.-F.; Ye, J.-R.; Song, W.; Jia, J.; Shen, Q. *J. Appl. Polym. Sci.* **2014**, *131*, 1.
8. Mendes, L. C.; Mallet, I. A.; Cestari, S. P.; Dias, F. G. *Polímeros* **2014**, *24*, 422.
9. Ujhelyiová, A.; Bolhová, E.; Marcinčin, A.; Tiňo, R. J. *Fiber Text. Eastern Eur.* **2007**, *15*, 26.
10. Szostak, M. *Molecular Cryst. Liq. Cryst.* **2004**, *416*, 209.
11. Di Lorenzo, M. L.; Errico, M. E.; Avella, M. *J. Mater. Sci.* **2002**, *37*, 2351.
12. Wu, D.; Lin, D.; Zhang, J.; Zhou, W.; Zhang, M.; Zhang, Y.; Wang, D.; Lin, B. *Macromol. Chem. Phys.* **2011**, *212*, 613.
13. Li, L.; Mao, L.; Duan, X. *Mater. Res. Bull.* **2006**, *41*, 541.
14. Tchmutin, I. A.; Ponomarenko, A. T.; Krinichnaya, E. P.; Kozub, G. I.; Efimov, O. N. *Carbon* **2003**, *41*, 1391.
15. Radhakrishnan, S.; Sonawane, P.; Pawashar, N. *J. Appl. Polym. Sci.* **2004**, *9*, 615.
16. Garbev, K.; Bornefeld, M.; Beuchle, G.; Stemmermann, P. *J. Am. Ceram. Soc.* **2008**, *91*, 3015.
17. Beuchle, G.; Garbev, K.; Bornefeld, M.; Black, L.; Stemmermann, P. *J. Am. Ceram. Soc.* **2008**, *91*, 3005.
18. Skinner, L. B.; Chae, S. R.; Benmore, C.; Wenk, H. R.; Monteiro, P. J. M. *Phys. Rev. Lett.* **2010**, *104*.
19. Grangeon, S.; Claret, F.; Linard, Y.; Chiaberge, C. *Acta Crystallogr., Sect. B: Struct. Sci. Cryst. Eng. Mater.* **2013**, *69*, 465.
20. Reynolds, R. C., *Clays Clay Miner.* **1986**, *34*, 359.

SGML and CITI Use Only
DO NOT PRINT